information

Article

Particle Swarm Optimization-Based Control for Maximum Power Point Tracking Implemented in a Real Time Photovoltaic System

Asier del Rio *, Oscar Barambones *, Jokin Uralde, Eneko Artetxe and Isidro Calvo

Department of Systems Engineering and Automatic Control, Faculty of Engineering of Vitoria-Gasteiz, University of the Basque Country (UPV/EHU), 01006 Vitoria-Gasteiz, Spain; jokin.uralde@ehu.eus (J.U.); eneko.artetxe@ehu.eus (E.A.); isidro.calvo@ehu.eus (I.C.)
* Correspondence: asier.delrio@ehu.eus (A.d.R.); oscar.barambones@ehu.eus (O.B.)

Abstract: Photovoltaic panels present an economical and environmentally friendly renewable energy solution, with advantages such as emission-free operation, low maintenance, and noiseless performance. However, their nonlinear power-voltage curves necessitate efficient operation at the Maximum Power Point (MPP). Various techniques, including Hill Climb algorithms, are commonly employed in the industry due to their simplicity and ease of implementation. Nonetheless, intelligent approaches like Particle Swarm Optimization (PSO) offer enhanced accuracy in tracking efficiency with reduced oscillations. The PSO algorithm, inspired by collective intelligence and animal swarm behavior, stands out as a promising solution due to its efficiency and ease of integration, relying only on standard current and voltage sensors commonly found in these systems, not like most intelligent techniques, which require additional modeling or sensoring, significantly increasing the cost of the installation. The primary contribution of this study lies in the implementation and validation of an advanced control system based on the PSO algorithm for real-time Maximum Power Point Tracking (MPPT) in a commercial photovoltaic system to assess its viability by testing it against the industry-standard controller, Perturbation and Observation (P&O), to highlight its advantages and limitations. Through rigorous experiments and comparisons with other methods, the proposed PSO-based control system's performance and feasibility have been thoroughly evaluated. A sensitivity analysis of the algorithm's search dynamics parameters has been conducted to identify the most effective combination for optimal real-time tracking. Notably, experimental comparisons with the P&O algorithm have revealed the PSO algorithm's remarkable ability to significantly reduce settling time up to threefold under similar conditions, resulting in a substantial decrease in energy losses during transient states from 31.96% with P&O to 9.72% with PSO.

Keywords: Particle Swarm Optimization (PSO); Maximum Power Point Tracking (MPPT); photovoltaic panels; P&O; nonlinear control; boost converter; renewable energies

Citation: del Rio, A.; Barambones, O.; Uralde, J.; Artetxe, E.; Calvo, I. Particle Swarm Optimization-Based Control for Maximum Power Point Tracking Implemented in a Real Time Photovoltaic System. *Information* **2023**, *14*, 556. https://doi.org/10.3390/info14100556

Academic Editors: Vasco N. G. J. Soares, João M. L. P. Caldeira, Bruno Bogaz Zarpelão and Jaime Galán-Jiménez

Received: 11 September 2023
Revised: 5 October 2023
Accepted: 9 October 2023
Published: 11 October 2023

1. Introduction

In recent decades, there has been a significant shift in energy production policies towards renewable sources [1], marking a paradigmatic change. This transition is driven by two key factors. Firstly, the global increase in energy consumption is projected to rise by 25% by 2040 [2,3]. To meet this growing demand, renewable energy sources are crucial, given the upward trajectory of oil prices [4]. Steps in this direction are being made, as the global renewable electricity capacity is expected to double the the capacity installed in the last 2 decades within the next 5 years [5]. Secondly, there is a growing awareness of the impact of climate change, where renewable energy sources, as the primary alternative, play a vital role. The International Plant Protection Convention forecast a climate scenario for 2050, indicating a potential global surface temperature rise of 1.5 °C to 2 °C unless significant reductions in CO_2 emissions are achieved in the coming decades [6]. Consequently, according to the latest report by the International Energy Agency, renewable

energy sources need to cover at least 70%, with half of this contribution expected to come from wind and solar power [7].

In this context, photovoltaic panels (PV) represent a simple and cost-effective solution [8]. Their benefits include zero emissions, the absence of moving mechanical parts, noise-free operation, low maintenance, and long lifespan [9,10]. All these factors, along with economic incentives and significant advances in electronics, greatly favor the development of photovoltaic panels as an energy source, making it one of the fastest-growing industries in renewable energy in recent years [11]. Regarding technical specifications, a photovoltaic system consists of multiple solar cells made of semiconductor materials, which absorb photons and generate a pair of electrons and holes through a p–n junction [12]. This process, involving electron diffusion to produce voltage, is intricate due to the limitation in capturing the full spectrum of sunlight [13]. As a result, the photovoltaic conversion efficiency generally remains below 20% [14].

Given the relatively low efficiency of a photovoltaic system, MPPT is an essential step as it helps the system achieve the best overall performance [15]. This can be achieved through a designed control technique that can be incorporated into a DC–DC converter [16,17]. However, PV cells, as well as PV modules, strings, and arrays, are characterized by a nonlinear power-voltage (P-V) curve that depends on incident irradiance [18], cell temperature [19] and, when present, partial shading [20]. As a result, one of the fundamental problems in photovoltaic generators is how to operate them at their MPP [21]. However, choosing an appropriate MPPT technique can be challenging due to the extensive number of proposed options, each with its own advantages and disadvantages. Primarily, there are two types of MPPT trackers: mechanical and electrical [21]. Mechanical trackers, also known as "solar trackers", can increase energy production by 17.72% to 31.23% [22]. However, this configuration is recommended for industrial applications, rather than residential ones, due to the excessive cost of mechanical tracking devices [23,24].

On the other hand, electrical MPPT techniques rely on power-voltage and current-voltage curves to track the optimal operating point. Electrical techniques can be classified into three main groups: offline MPPT techniques, online MPPT techniques or Hill Climbing, and intelligent MPPT techniques [21]. Offline techniques are based on estimating the MPP by systematically exploring various combinations of voltage and current. These techniques employ algorithms and mathematical models to determine the optimal operating point. On the other hand, Hill Climbing techniques perform real-time tracking of the MPP by incrementally adjusting the voltage or current of the solar panel and evaluating whether the generated power increases or decreases. This process is repeated until the maximum power point is reached [25]. These techniques are widely used due to their ease of implementation and reduced cost, although they have limitations in terms of performance and difficulties in reaching the MPP under adverse environmental conditions [26]. A classification of MPPT techniques can be found in [27,28].

In comparison to offline and online MPPT methods, intelligent MPPT techniques, while requiring higher computational costs, offer better accuracy and tracking efficiency with fewer oscillations in steady-state. Additionally, unlike offline and online techniques, intelligent methods can track the global MPP under partial shading conditions [29].

One of the intelligent techniques that has gained popularity in various fields in recent years is the Particle Swarm Optimization (PSO) technique. This algorithm is an optimization technique based on collective intelligence and the behavior of swarms of particles. It draws inspiration from observed movement patterns in groups of animals, such as migratory birds or schooling fish [30]. In PSO, a set of particles is represented in a multidimensional space, where each particle seeks the optimal solution through iteration and communication with other particles [31].

The advantage of PSO is that it can be easily implemented in any installation that is already using Hill Climbing algorithms, which are the most commonly used methods in the field of MPPT. This is possible because, like Hill Climbing algorithms, PSO only requires current and voltage sensors typically included in converters and a microprocessor in order

to implement the MPPT algorithm [32]. This provides a significant advantage over other intelligent algorithms, which often require additional sensors to measure environmental conditions, high processing power, or a preliminary study of the system in which they will operate, thus increasing the installation and maintenance costs and time of the plants [33].

The primary contribution of this study lies in the implementation and validation of an advanced control system based on the PSO algorithm for real-time Maximum Power Point Tracking (MPPT) in a commercial photovoltaic system to assess its viability by testing it against the industry-standard controller, Perturb and Observe (P&O), to highlight its advantages and limitations. This is significant because, despite being validated by multiple researchers in simulations, comparisons in commercial systems against industry-standard controllers are not usually established, which are still largely operating with non-intelligent controls. We selected the PSO algorithm from among all possible proposals due to its ease of implementation in commercial installations that have traditional control systems, such as a P&O algorithm. This is particularly attractive, as it would greatly facilitate the transition from the use of traditional controllers to more effective intelligent controllers, potentially increasing the performance of these generators.

This paper is structured as follows: Section 2 describes the hardware used and its interconnection, as well as further details about the controllers handled for the MPPT tracking. Section 3 presents the outcomes gathered with the implemented controllers. Finally, Section 4 comprises a summary of the highlights accomplished throughout this research.

2. Materials and Methods

2.1. Hardware Description

The proposed control structures were implemented in real-time using commercial hardware for validation. The employed photovoltaic panel was a Peimar SG340P polycrystalline solar panel which arranges 72 high-quality module cells in a 12 × 6 array. The panel is protected by a low-iron tempered glass front cover and a double-wall aluminum frame for mechanical stiffness. These panels are commonly used in commercial, residential, and industrial environments due to their light weight, robustness, high rigidity and convenient installation. The characteristics of the Peimar SG340P are gathered in Table 1.

Table 1. Technical data of SG340P panel.

Properties	Values	Units
Dimensions	156 × 156	mm
Number of series cells	6	units
Number of parallel cells	12	units
Maximum Power	340	W
Max. Power Voltage	37	V
Max. Power Current	9	A
Open-circuit voltage	45	V
Short-Circuit Current	9.9	A

Although it is not necessary for the operation of the controllers, it is convenient to know the effects of the environmental variables during the experiments. Temperature and radiation were monitored using a trustworthy external silicon sensor, specifically the Ingenieurbüro Si-V-10TC-T. This sensor is specifically designed for accurately measuring photovoltaic variables. It consists of a monocrystalline silicon solar cell connected to a transducer. Additionally, it incorporates an active temperature compensator located on the rear surface of the module, which effectively corrects measurements and provides supplementary temperature information. The measured signals are transmitted as voltage variations within the 0–10 V range. For more detailed information, please refer to Table 2.

Table 2. Ingenieurbüro Si-V-10TC-T specifications.

Properties	Values	Units
Voltage Supply	12 to 28	V_{D_C}
Temperature Measurement Range	−40 to 90	°C
Irradiance Measurement Range	0 to 1500	W/m^2

In order to adjust the electrical outputs of the PV panel, a TEP-192 boost converter produced by the research group at the University of Huelva has been implemented. This device operates with a 20 kHz PWM switching input signal and provides information of the electrical variables as 0–10 V output analog signals for monitoring. The module incorporates two Schottky diodes, MURF1560 GT, two capacitances, TK (1.5 mF and 3 mF), six PVC2-564-08 inductances, and an IGBT, HGT40N60B3. Voltage and current readings are provided in 0–10 V signals. Additional technical data about this converter is described in Table 3.

Table 3. TEP-192 specifications.

Properties	Values	Units
Switching frequency	20	kHz
Max. input voltage	60	V
Max. input current	30	A
Max. output voltage	250	V
Max. output current	30	A

To complete the electrical circuit, a BK Precision model 8500B was used. This is a programmable DC load with broad flexibility and suitability for testing and evaluating DC power sources, especially photovoltaic panels. This programmable resistance includes several useful features such as reverse polarity protection, which avoids overheating, power, voltage, and current overload on the PV system. Its characteristics are shown in Table 4.

Table 4. BK8500 specifications.

Properties	Values	Units
Max. Power Rating	300	W
Operating voltage	0–120	V
Max Current Rating	30	A
Load range	0.1–4000	Ω

The generation of the PWM signal was accomplished through the utilization of dSPACE's DS1202 MicroLabBox hardware, specifically designed for software development and validation. This versatile hardware is capable of generating analog, digital, and PWM signals. Powered by a programmable FPGA equipped with a dual-core processor, it offers impressive specifications including clock speeds of up to 2 GHz, 1 GB of DRAM, and 128 MB of flash memory. The device also features Real-Time Interface (RTI), a platform that facilitates the rapid and automatic generation of C code, allowing designers to concentrate their efforts on the Simulink interface. Furthermore, dSPACE's ControlDesk tool provides a comprehensive solution for visualizing measured variables and enables the manipulation of control signals.

Figure 1 shows a diagram representing the hardware described and its connections between the elements.

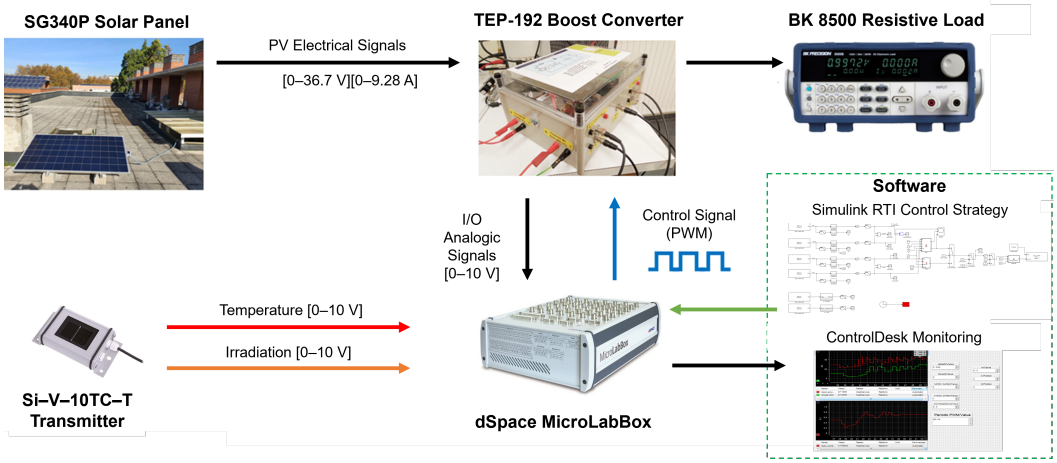

Figure 1. Hardware–software workflow diagram.

2.2. Maximum Power Point (MPP)

Tracking the maximum power point is essential to ensure that the photovoltaic system operates at its highest efficiency at all times. MPPT techniques are necessary to continuously track and adjust the operational parameters of the system, such as voltage or current, to maximize power production, which has become an industry standard. This is achieved through algorithms that control and optimize the system's operating points based on solar radiation and the electrical characteristics of the solar panels, for example, by influencing the behavior of a DC–DC converter that adjusts the electrical characteristics of the panel [34].

In addition to optimizing power production, MPPT plays a crucial role in enhancing the overall performance and longevity of photovoltaic systems. By dynamically adapting to variations in solar radiation and environmental conditions, MPPT helps improve system stability and reliability. Whether it is coping with changing weather patterns, adjusting to partial shading scenarios, or managing varying panel temperatures, MPPT ensures that the photovoltaic system operates at or near its maximum power point. This capability minimizes energy losses and maximizes energy yield, even under challenging conditions [35].

Furthermore, the importance of MPPT becomes evident when examining characteristic power-voltage curves, as shown in Figure 2. These curves illustrate how delivered power varies depending on factors such as the resistive load value, incident radiation, panel temperature, and partial shading conditions. MPPT enables the system to navigate these complex and dynamic conditions effectively, ensuring that it consistently delivers optimal performance and energy production. This capability is vital for both grid-connected and off-grid photovoltaic installations, where energy efficiency and reliability are paramount for sustainable power generation and reducing environmental impact.

2.3. Particle Swarm Optimization (PSO) Controller

The PSO algorithm is part of the bio-inspired algorithms, which draw inspiration from the behavior of bird flocks and other animals and how they interact and move in search of resources [36]. Proposed by Kennedy and Eberhart in 1995 [37,38], this algorithm is suitable for solving a wide range of optimization problems, including the one addressed in this study. In the original algorithm, a search space encompassing all possible solutions is defined, along with a population of particles representing potential solutions. These potential solutions are evaluated using the objective function and, iteration by iteration, converge towards the best solution.

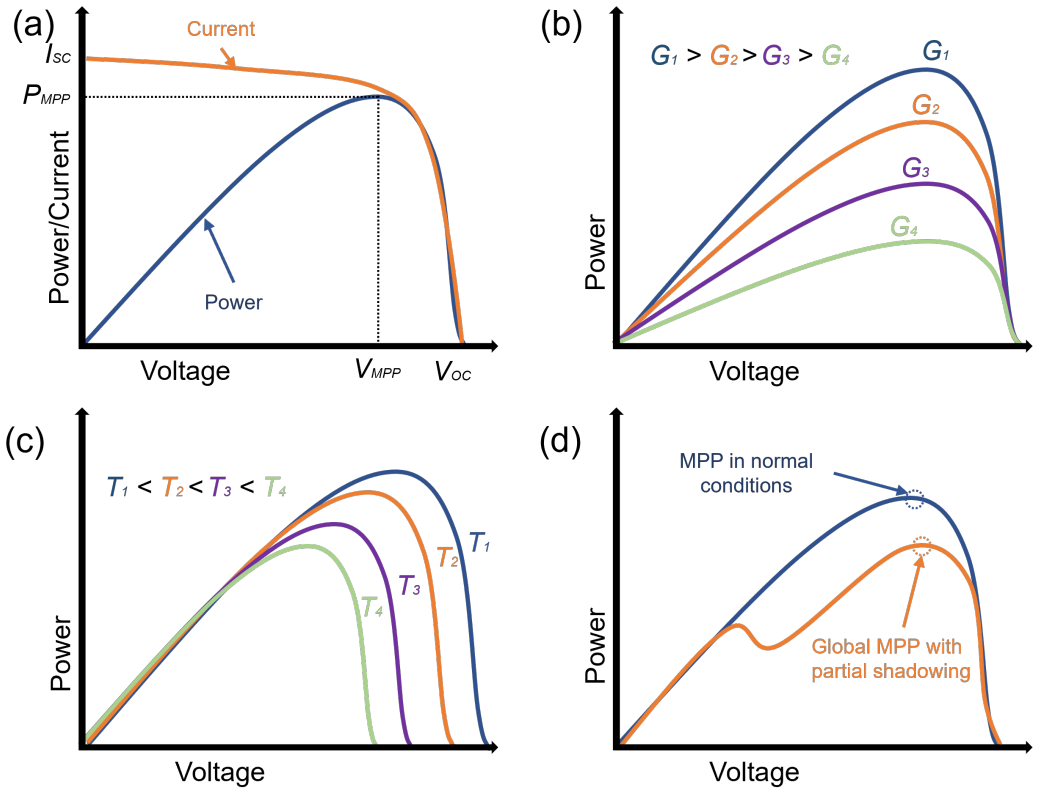

Figure 2. Electrical curves of a photovoltaic system, where: (**a**) is a conventional power vs. voltage and power vs. current graph with the MPP highlighted; (**b**) displays the variation in power-voltage curves with constant temperature and variable irradiation; (**c**) illustrates how power-voltage curves change with different temperatures at constant irradiation; (**d**) demonstrates the impact of partial shading on power vs. voltage curves.

The algorithm operates as follows: it starts with a population of particles whose initial positions are randomly chosen within defined boundaries. In each iteration, each particle calculates its velocity V_i based on its previous velocity, its previous best personal position, P_{best_i} and the best global position found so far, G_{best}, according to Equation (1). Then, each particle position is updated with its current position and the calculated velocity, as shown in (2). These optimal values are determined based on the power generated by each particle compared to the maximum power found so far [39,40].

$$V_i(k+1) = W \cdot V_i(k) + C_1 \cdot rand_1 \cdot (P_{best_i}(k) - X_i(k)) + C_2 \cdot rand_2 \cdot (G_{best}(k) - X_i(k)) \quad (1)$$

$$X_i(k+1) = X_i(k) + V_i(k+1) \quad (2)$$

where C_1 is the acceleration component associated with P_{best}, C_2 is the acceleration component associated with G_{best}. Modifying these coefficients allows for adjusting the desired behavior in the algorithm. Giving more weight to the C_1 coefficient will result in a more exploratory behavior, while giving weight to the C_2 coefficient will exploit the best solution more [41]. Finally, W represents the weight or inertia of the particle, $rand_1$ and $rand_2$ are random numbers between 0 and 1. The inclusion of this randomness, along with the exploration of the search space, allows the PSO algorithm to converge towards the global maximum and avoid being trapped in local maxima. This exploration of the search space is depicted in Figure 3.

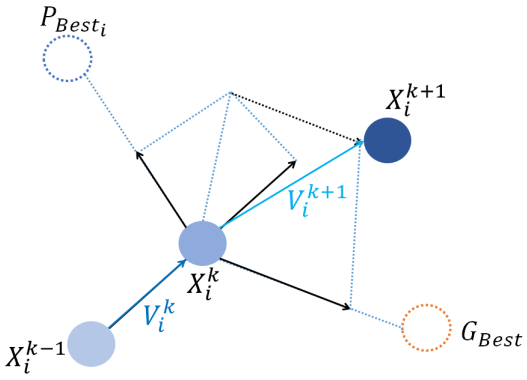

Figure 3. Representation of the particle movement in the search space of the PSO algorithm.

In the context of MPPT, the particles in PSO represent different points on the power vs. voltage curve of a PV, as illustrated in Figure 4:

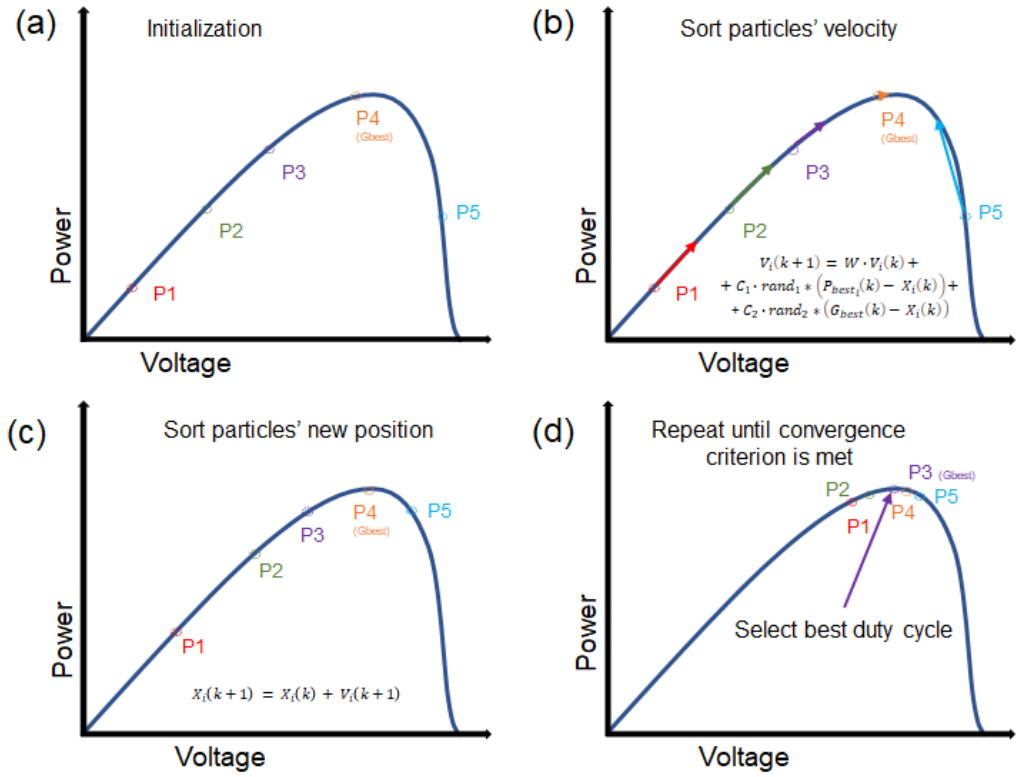

Figure 4. Representation of particle movement during the execution of the PSO algorithm: (**a**) initialization of particles, (**b**) calculation of particle velocities V_i, (**c**) calculation of new particle positions X_i, (**d**) particle positions when the convergence criterion is met.

Each particle has a position and velocity in the search space, which corresponds to a set of current and voltage values, related to a duty cycle [42]. On the other hand, the objective function is not a mathematical function; instead, in each iteration, the solution proposed by a particle (its duty cycle value) is applied, and the extracted power is determined. The full operation of the implemented controller is depicted in Figure 5 as a flowchart:

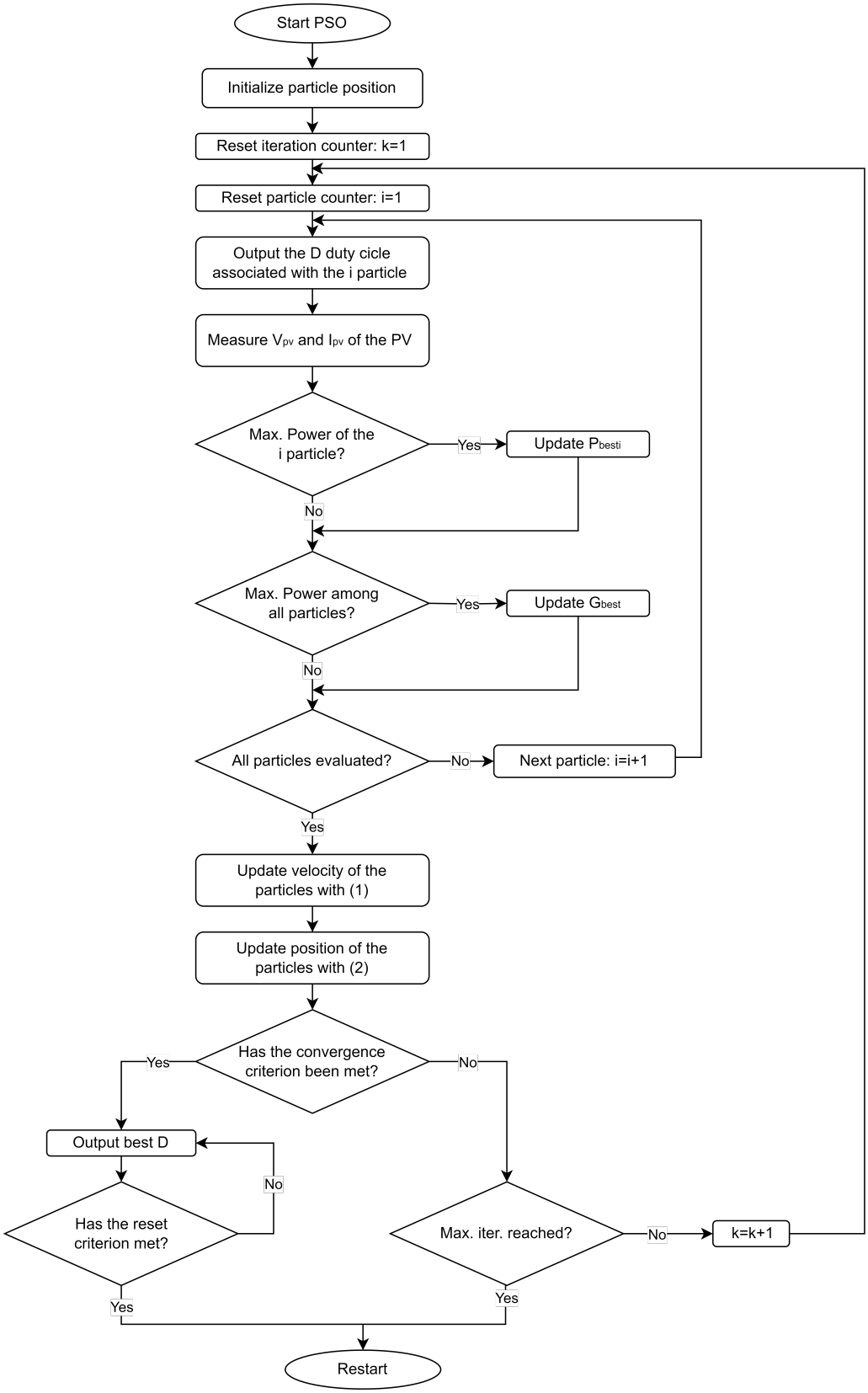

Figure 5. Flowchart illustrating the operation of the PSO algorithm.

As the flowchart describes, initially, and whenever the algorithm is restarted, the particle positions are randomly initialized throughout the operation range of the duty cycle of the boost converter, 0.1 to 0.9 in this particular case. Likewise, the velocities of the particles is initialized as zero. Then, in each k iteration, the the output power related to each particle position is measured, outputting the duty cycle associated with each i particle. In case the read power value of the i particle is greater than all the previous ones read by that i particle, the best personal position P_{best_i} of the i particle is saved. Likewise, if the read power value of any particle is greater than all the previous ones read by every particle, the best global position G_{best} is saved. At the end of every k iteration, when all the particles have been evaluated, the velocity and positions of every particle is updated according to the (1) and (2) equations. This process is repeated until the convergence criterion is met. Each user is free to establish their desired criterion. In the experiments conducted in this research, the chosen criterion was that every particle has to be at most 5% apart from each other in the selected operating range of the duty cycle. Once this criterion is fulfilled, the best found solution, e.g., the duty cycle founded which produces the greater power is established as the output of the controller. The algorithm will keep that output until the reset criterion is met. When that happens, the algorithm will restart the search. Again, each user is free to establish their desired criterion for the reset of the algorithm. Ideally, it has to be one that reflects a meaningful change on the power output, which is usually lead by a sudden change in the incident radiation. In the experiments conducted, the chosen criterion was that the output power of the system varies more than 1% compared to the power output when the algorithm converged. Finally, a maximum of 50 iterations has been set for the unlikely scenario in which the algorithm does not converge, so that it can be restarted.

2.4. Perturb and Observe (P&O) Controller

The P&O algorithm, known for its simplicity, is one of the most widely used methods for MPPT in PV systems, and is the reason for which it has been chosen as a reference point for the validation of the proposed PSO controller. Its ease of implementation and low cost make it appealing in the industry [43]. This algorithm operates by perturbing the duty cycle, which increases or decreases the output power of the photovoltaic panel, and then comparing this power with the previous system state, as shown in Figure 6. When the perturbation is produced, the power changes. If the new power is greater than the previous power, the perturbation moves again in the actual direction; otherwise, it moves in the opposite direction. This process continues until the maximum power is reached. Figure 7 illustrates the flowchart of the algorithm.

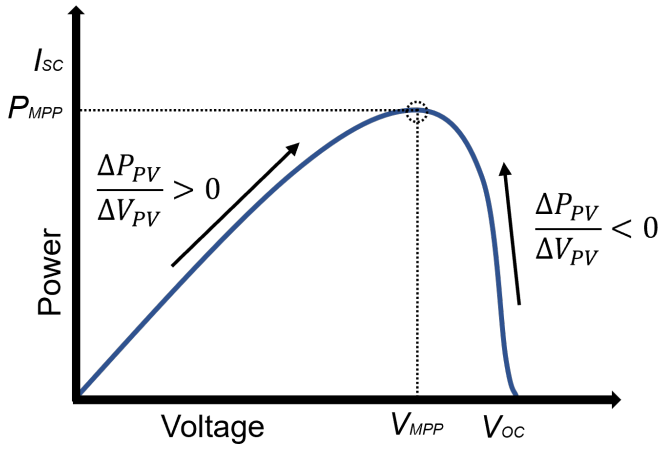

Figure 6. Operation concept of the P&O algorithm.

Although this conventional method is widely used due to its simplicity, it has some limitations. One limitation is the oscillation of the operating point around the desired MPP during tracking [32,43]. After reaching the MPP, the power oscillates around the maximum, which reduces the power output of the photovoltaic system. One way to dampen this oscillation is by reducing the perturbation size. This increases accuracy and dampens the power oscillation of the photovoltaic system at the expense of reducing the algorithm's tracking speed [44]. In this situation, a larger number of iterations are required to reach the MPP, resulting in more time being needed and, therefore, more power loses until the system reach the MPP.

Another limitation of the P&O algorithm is its slow response to changes in environmental conditions and partial shading conditions, where multiple peaks exist in the P vs. V curve, leading to deviations from the exact MPP because the P&O algorithm cannot distinguish between a local maximum and a global maximum so, unfortunately, this algorithm forces the system state to the first maximum (global or local) that is reached [43].

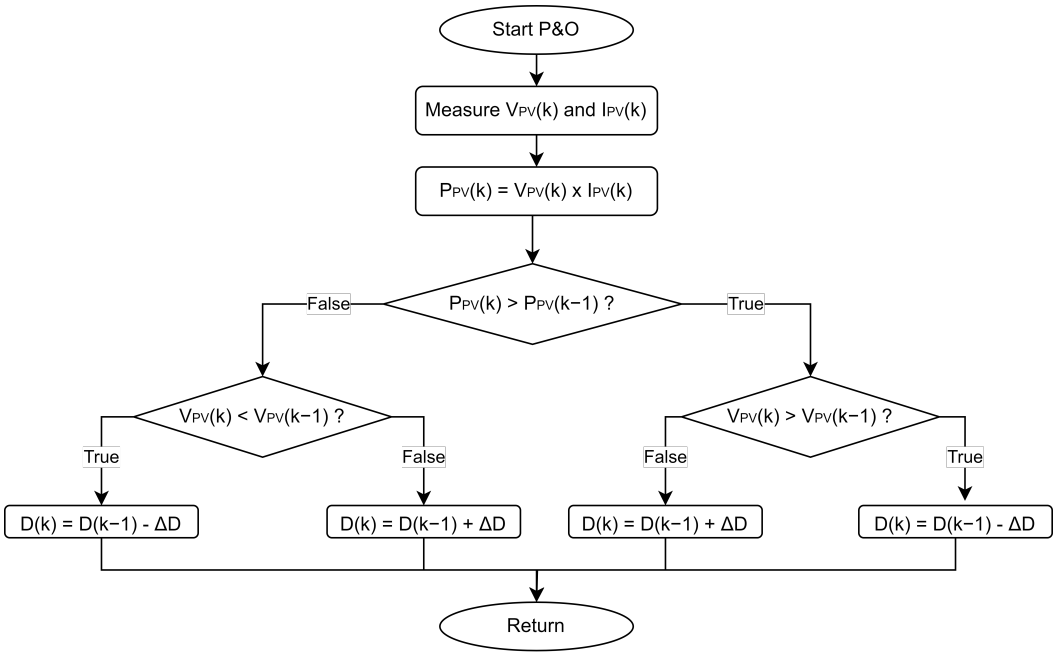

Figure 7. Flow chart of the P&O controller.

3. Results

3.1. Sensibility Analysis of the W, C_1 and C_2 Parameters

Just like in other types of controllers, the PSO-type controller has several parameters that can be adjusted by the user to determine its desired dynamics. In this case, the parameters to be adjusted are the three constants present in the equation governing the position of a new particle (1). Tuning these three weighting coefficients results in different static and dynamic behaviors of the controller.

The combination of these three parameters, W, C_1 and C_2, gives rise to three main possible combinations, depending on which one is the most weighted. For example, if the inertia parameter is primarily weighted ($W = 1$; $C_1 = C_2 = 0$), the direction in which the particle moves in the workspace never changes and continues increasing or decreasing until reaching the maximum or minimum limits of the duty cycle. This causes the photovoltaic system to never reach the MPP and never converge.

On the other hand, if the C_1 parameter is primarily weighted ($C_1 = 1$; $W = C_2 = 0$), the new duty cycle value of the i-th particle converges towards the best local duty cycle P_{best_i}. This choice makes each particle insensitive to the global optimal position.

Finally, if the C_2 parameter is primarily weighted ($C_2 = 1$; $W = C_1 = 0$), all particles converge towards the first-best global duty cycle G_{best} without exploring the search space.

For these reasons, a sensitivity analysis must be conducted to determine the most effective combination of the three parameters. To do this, an experiment has been performed by testing different combinations of PSO parameters, with an identical load (140 Ω) and radiation conditions as similar and constant as possible, around 900–1100 W/m^2. Four sets of parameters have been established, as shown in Table 5, and the experiment results are presented in Figure 8. To avoid influencing the tuning of these parameters, a fixed number of particles has been selected for all sets. The choice has been made to use five of them since, during testing, it has been observed that they provide the best trade-off between exploring the search space and convergence time.

Table 5. Sets of the PSO parameter sensitivity analysis experiment.

Sets	W	C_1	C_2
1	0.3	0.3	0.3
2	0.3	1	0.2
3	1	0.3	0.2
4	0.2	0.2	0.6

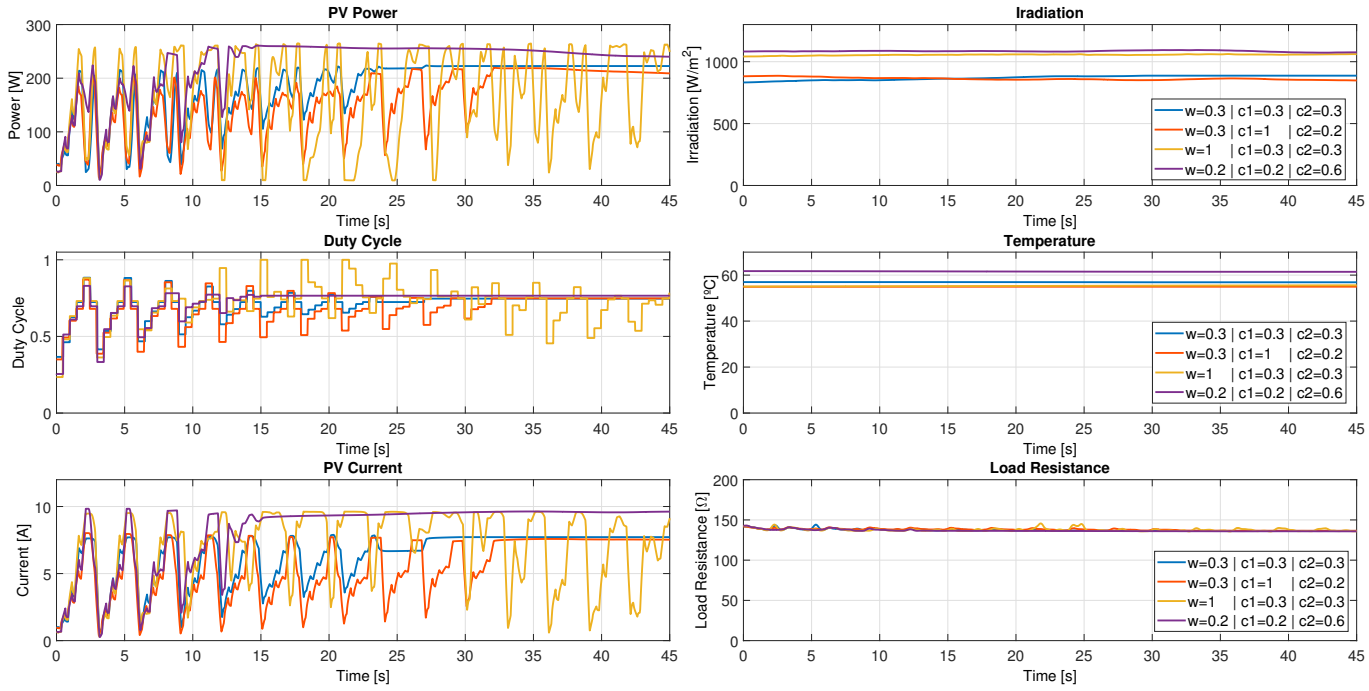

Figure 8. Results of the sensitivity analysis of the W, C_1 and C_2 parameters.

To assess the efficiency and effectiveness of each set, two indicators will be calculated: the algorithm convergence time, t_c, and the energy loss, E_L, during the transient state $[t_0, t_c]$. The latter indicator, along with its normalized version, is calculated as shown in Equations (3) and (4):

$$E_L = \int_{t_0}^{t_c} |P_c - P(t)| dt \tag{3}$$

$$E_L(\%) = \frac{E_L}{E_{tot}} \cdot 100 \tag{4}$$

where P_c is the power at the MPP found by the algorithm, $P(t)$ is the instantaneous power, and E_{tot} is the total energy that would have been extracted if the algorithm had remained at the MPP found throughout the entire experiment. The results of these comparisons are presented in Table 6.

Table 6. Performance comparison between different PSO parameter sets.

Sets	W	C_1	C_2	D_c	P_c [W]	E_L (%)	t_c [s]
1	0.3	0.3	0.3	0.7466	222.37	16.79	26
2	0.3	1	0.2	0.7482	219.47	26.97	32
3	1	0.3	0.2	-	259.04	35.83	-
4	0.2	0.2	0.6	0.7656	260.46	10.89	15

Analyzing the results, it is observed that the PSO with parameters adjusted using Set 4 achieves both a lower convergence time and a smaller energy loss during transient states, making it the clear winner.

From the experiment, it can be concluded that the most appropriate parameters for MPPT are those that favor convergence towards the global maximum in each iteration, i.e., those that weigh the C_2 parameter more, resulting in a lower convergence time. Additionally, they maintain the exploration of the search space with a lower, yet significant weighting of the other parameters.

Therefore, the tuning parameter values for the PSO-based controllers used in the experiments carried out in this paper have been established as: $W = 0.2$; $C_1 = 0.2$; $C_2 = 0.6$.

3.2. Performance Comparison: PSO vs. P&O

In this section, a comparison of operation and performance is conducted between the PSO and the P&O algorithm to determine the improvement provided by the proposed new algorithm. The P&O algorithm was chosen due to its widespread usage in the industry for photovoltaic power generation systems. Additionally, both algorithms require the same electrical sensors to operate, namely the voltage and current measurements from the panel at each moment. They do not require any radiation or temperature sensors, nor do they rely on any reference voltage estimators (VRE). This allows the PSO algorithm to be installed in applications where a P&O algorithm is already in place, without incurring significant expenses or requiring additional hardware installations. This potential for enhanced performance makes the P&O algorithm a reasonable benchmark for evaluating the performance of the proposed algorithms.

Due to its operation, the dynamic behavior of this algorithm is directly influenced by the increment/decrement applied to the duty cycle at each iteration (ΔD). Generally, a small increment is preferred, as when the algorithm reaches the vicinity of the MPP, it tends to oscillate continuously, resulting in a stationary state with oscillations that never fully reaches the MPP. A small ΔD mitigates this issue at the expense of relatively longer convergence times. Additionally, if a local maximum is encountered between the MPP and the current operating duty cycle of the P&O algorithm, it will inevitably fall into it.

Taking into account the previous considerations, an experiment was conducted to compare the performance of the PSO algorithm against the P&O algorithm. For this purpose, radiation conditions were kept as constant as possible (around 1000 W/m^2), and three tests were performed: one with the PSO algorithm and two with the P&O algorithm. The latter two tests differed in terms of ΔD. The first P&O test used a small increment of $\Delta D = 0.005$ to observe the normal dynamics of P&O, while the second test used a larger increment of 0.025 to achieve faster dynamics for comparison. For all algorithms, an iteration was performed every 0.5s. The results of the experiment are shown in Figure 9. Furthermore, Table 7 presents the settling times and energy performance of these algorithms in the experiment.

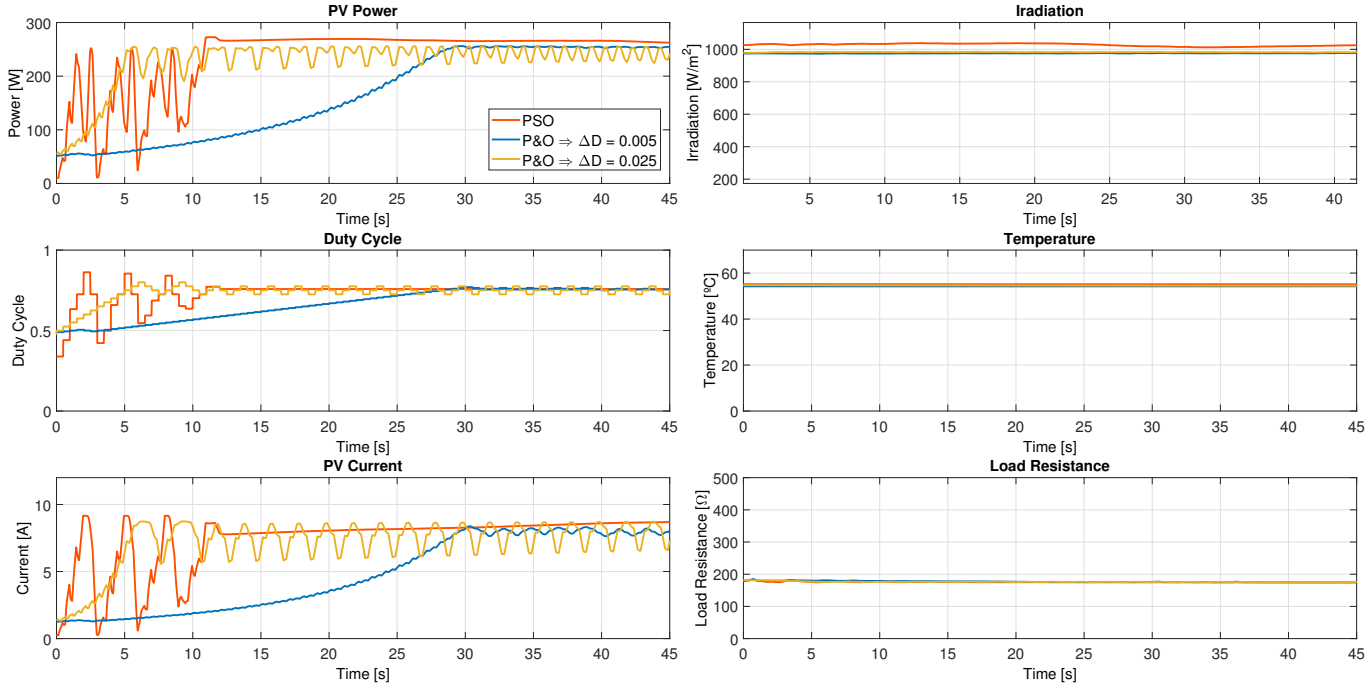

Figure 9. Results of the PSO vs. P&O performance experiment.

Table 7. Performance comparison between PSO and P&O controllers.

Algorithm	ΔD	D_c	P_c [W]	E_L (%)	t_c [s]
PSO	-	0.7579	264.35	9.72	12
P&O	0.005	0.755–0.765	255.924	31.96	31
P&O	0.025	0.725–0.775	254.27	13.18	7

Regarding the dynamics of the transient state, it is observed that the PSO algorithm finds the MPP almost three times faster than the P&O algorithm with a small step, and it exhibits significantly lower energy losses, reducing them from 31.96% to 9.72%. On the other hand, the P&O algorithm with a larger step has a shorter convergence time than the PSO but also bigger (3.46%) energy losses. It is important to note that the energy loss is calculated only within the 45 s duration of the experiment. If the test were extended for a longer period, the poor response exhibited by the P&O algorithm during steady state conditions would likely result in even worse energy losses.

Regarding the behavior during the steady state, it is observed that the PSO algorithm remains stable without oscillations, while the P&O algorithm exhibits oscillations, never fully reaching the MPP. This oscillation is moderate and acceptable with a small ΔD but becomes unacceptable with the larger step, as shown in the figure.

Taking all factors into account, it can be concluded that the PSO algorithm demonstrates superior performance compared to the P&O controller in terms of convergence time, behavior in steady-state, and energy efficiency.

4. Conclusions and Future Work

In this study, the use of an advanced control system based on the Particle Swarm Optimization algorithm for Maximum Power Point Tracking in real photovoltaic systems is summarized. After designing the controller based on the PSO algorithm, a sensitivity analysis of the parameters governing the search dynamics of the algorithm was performed to determine the most effective combination for real-time MPPT. The experiments demonstrated that a combination favoring exploitation behavior resulted in more advantageous dynamics of convergence, leading to faster convergence and more precise solutions.

Once the controller was properly tuned, several experiments were conducted to test its performance. A P&O controller was selected as a reference since it is one of the most popular algorithms in the photovoltaic industry. Additionally, the P&O algorithm requires the same sensors as the PSO algorithm to operate, making the comparison between both algorithms interesting, as the proposed new control could be integrated into existing P&O-based installations without additional costs. The comparative experiment demonstrated that the PSO algorithm significantly reduces the settling time from 31 s to only 12 s under similar conditions, resulting in a decrease in energy losses during transient states from 31.96% with P&O to 9.72% with PSO. Therefore, it can be stated that the PSO algorithm outperforms its counterpart, proving to be a promising improvement for solar energy generation systems.

The validation of this controller in a commercial panel represents an advancement in the state of the art in MPPT algorithms. Progress in this type of algorithm can facilitate the incorporation of intelligent control in commercial systems since, unlike other intelligent algorithms, PSO-based controllers do not require additional sensorization, specific component modeling, or high computing capacity to function. These factors, which tend to increase installation and maintenance costs, make these alternatives undervalued by the industry.

Despite the promising results and the experience gained during the development of the algorithm and the conducted experiments, certain characteristics have potential for improvement. The PSO algorithm is a general optimization algorithm applicable to a multitude of situations. However, certain modifications can be made to enhance its performance for this specific application. In future studies, variants of the algorithm could be tested to improve the original algorithm's performance by incorporating domain-specific knowledge. Similarly to other cases, bounded particle initializations could be proposed to enhance the dynamic characteristics of the search phase. Additionally, the inclusion of selection mechanisms to aid particle convergence and exploration of alternative convergence criteria would be interesting avenues for exploration.

Author Contributions: Conceptualization, A.d.R. and O.B.; methodology, A.d.R., O.B., E.A. and J.U.; investigation, A.d.R.; writing—original draft preparation, A.d.R.; writing—review and editing, A.d.R., O.B., E.A. and J.U.; visualization, A.d.R., E.A. and J.U.; supervision, O.B. and I.C.; project administration, O.B. and I.C. All authors have read and agreed to the published version of the manuscript.

Funding: This research received no external funding.

Institutional Review Board Statement: Not applicable.

Informed Consent Statement: Not applicable.

Data Availability Statement: Data are available on request from the authors.

Acknowledgments: The authors wish to express their gratitude to the Basque Government, through the project EKOHEGAZ II, to the Diputación Foral de Álava (DFA), through the project CONAVANTER, and to the UPV/EHU, through the project GIU20/063 and MobilityLab Foundation (CONV23/14. Proy. 16), for supporting this work.

Conflicts of Interest: The authors declare no conflicts of interest.

References

1. IEA. Global Energy Investment in Clean Energy and in Fossil Fuels, 2015–2023. 2023. Available online: https://www.iea.org/data-and-statistics/charts/global-energy-investment-in-clean-energy-and-in-fossil-fuels-2015-2023 (accessed on 5 July 2023).
2. Vera, Y.E.; Dufo-López, R.; Bernal-Agustín, J.L. Energy management in microgrids with renewable energy sources: A literature review. *Appl. Sci.* **2019**, *9*, 3854. [CrossRef]
3. Gielen, D.; Boshell, F.; Saygin, D.; Bazilian, M.D.; Wagner, N.; Gorini, R. The role of renewable energy in the global energy transformation. *Energy Strategy Rev.* **2019**, *24*, 38–50. [CrossRef]
4. IEA. *Oil Market Report—April 2023*; Technical Report; International Energy Agency (IEA): Paris, France, 2023.

5. IEA. *Total Renewable Electricity Capacity Additions, 2001–2027*; IEA: Paris, France, 2022. Available online: https://www.iea.org/data-and-statistics/charts/total-renewable-electricity-capacity-additions-2001-2027 (accessed on 5 July 2023).
6. *Climate Change 2021: The Physical Science Basis*; Technical Report; International Panel on Climate Change: Geneva, Switzerland, 2021.
7. *Net Zero by 2050*; Technical Report; International Energy Agency: Paris, France, 2021.
8. Farhat, M.; Barambones, O.; Sbita, L. A new maximum power point method based on a sliding mode approach for solar energy harvesting. *Appl. Energy* **2017**, *185*, 1185–1198. [CrossRef]
9. Alsadi, S.; Khatib, T. Photovoltaic power systems optimization research status: A review of criteria, constrains, models, techniques, and software tools. *Appl. Sci.* **2018**, *8*, 1761. [CrossRef]
10. Adefarati, T.; Bansal, R.C. *Energizing Renewable Energy Systems and Distribution Generation*; Elsevier: Amsterdam, The Netherlands, 2019.
11. Sheng, R.; Du, J.; Liu, S.; Wang, C.; Wang, Z.; Liu, X. Solar photovoltaic investment changes across china regions using a spatial shift-share analysis. *Energies* **2021**, *14*, 6418. [CrossRef]
12. Kapsalis, V.; Kyriakopoulos, G.; Zamparas, M.; Tolis, A. Investigation of the photon to charge conversion and its implication on photovoltaic cell efficient operation. *Energies* **2021**, *14*, 3022. [CrossRef]
13. Dharmadasa, I.M.; Ojo, A.A.; Salim, H.I.; Dharmadasa, R. Next generation solar cells based on graded bandgap device structures utilising rod-type nano-materials. *Energies* **2015**, *8*, 5440–5458. [CrossRef]
14. Leitão, D.; Torres, J.P.N.; Fernandes, J.F. Spectral irradiance influence on solar cells efficiency. *Energies* **2020**, *13*, 5017. [CrossRef]
15. Gursoy, M.; Zhuo, G.; Lozowski, A.G.; Wang, X. Photovoltaic energy conversion systems with sliding mode control. *Energies* **2021**, *14*, 6071. [CrossRef]
16. Rasheduzzaman, M.; Fajri, P.; Kimball, J.; Deken, B. Modeling, analysis, and control design of a single-stage boost inverter. *Energies* **2021**, *14*, 4098. [CrossRef]
17. Cordeiro, A.; Chaves, M.; Gâmboa, P.; Barata, F.; Fonte, P.; Lopes, H.; Pires, V.F.; Foito, D.; Amaral, T.G.; Martins, J.F. Automated Solar PV Simulation System Supported by DC–DC Power Converters. *Designs* **2023**, *7*, 36. [CrossRef]
18. Yan, K.; Shen, H.; Wang, L.; Zhou, H.; Xu, M.; Mo, Y. Short-term solar irradiance forecasting based on a hybrid deep learning methodology. *Information* **2020**, *11*, 32. [CrossRef]
19. Villalva, M.G.; Ruppert, E. Analysis and simulation of the P&O MPPT algorithm using a linearized PV array model. In Proceedings of the 2009 35th Annual Conference of IEEE Industrial Electronics, Porto, Portugal, 3–5 November 2009; pp. 231–236. [CrossRef]
20. Nabulsi, A.A.; Dhaouadi, R. Efficiency optimization of a dsp-based standalone PV system using fuzzy logic and dual-MPPT control. *IEEE Trans. Ind. Inform.* **2012**, *8*, 573–584. [CrossRef]
21. Derbeli, M.; Napole, C.; Barambones, O.; Sanchez, J.; Calvo, I.; Fernández-Bustamante, P. Maximum power point tracking techniques for photovoltaic panel: A review and experimental applications. *Energies* **2021**, *14*, 7806. [CrossRef]
22. Bahrami, A.; Okoye, C.O.; Atikol, U. The effect of latitude on the performance of different solar trackers in Europe and Africa. *Appl. Energy* **2016**, *177*, 896–906. [CrossRef]
23. Ramful, R.; Sowaruth, N. Low-cost solar tracker to maximize the capture of solar energy in tropical countries. *Energy Rep.* **2022**, *8*, 295–302. [CrossRef]
24. Musa, A.; Alozie, E.; Suleiman, S.A.; Ojo, J.A.; Imoize, A.L. A Review of Time-Based Solar Photovoltaic Tracking Systems. *Information* **2023**, *14*, 211. [CrossRef]
25. Alaraj, M.; Kumar, A.; Alsaidan, I.; Rizwan, M.; Jamil, M. An Advanced and Robust Approach to Maximize Solar Photovoltaic Power Production. *Sustainability* **2022**, *14*, 7398. [CrossRef]
26. Troudi, F.; Jouini, H.; Mami, A.; Khedher, N.B.; Aich, W.; Boudjemline, A.; Boujelbene, M. Comparative Assessment between Five Control Techniques to Optimize the Maximum Power Point Tracking Procedure for PV Systems. *Mathematics* **2022**, *10*, 1080. [CrossRef]
27. Baba, A.O.; Liu, G.; Chen, X. Classification and Evaluation Review of Maximum Power Point Tracking Methods. *Sustain. Futures* **2020**, *2*, 100020. [CrossRef]
28. Ram, J.P.; Babu, T.S.; Rajasekar, N. A comprehensive review on solar PV maximum power point tracking techniques. *Renew. Sustain. Energy Rev.* **2017**, *67*, 826–847. [CrossRef]
29. Elobaid, L.M.; Abdelsalam, A.K.; Zakzouk, E.E. Artificial neural network-based photovoltaic maximum power point tracking techniques: A survey. *IET Renew. Power Gener.* **2015**, *9*, 1043–1063. [CrossRef]
30. Nickabadi, A.; Ebadzadeh, M.M.; Safabakhsh, R. A novel particle swarm optimization algorithm with adaptive inertia weight. *Appl. Soft Comput. J.* **2011**, *11*, 3658–3670. [CrossRef]
31. Charilogis, V.; Tsoulos, I.G. Toward an Ideal Particle Swarm Optimizer for Multidimensional Functions. *Information* **2022**, *13*, 217. [CrossRef]
32. Arif, M.S.B.; Mustafa, U.; bin Md. Ayob, S. Extensively used conventional and selected advanced maximum power point tracking techniques for solar photovoltaic applications: An overview. *AIMS Energy* **2020**, *8*, 935–958. [CrossRef]
33. Sharmin, R.; Chowdhury, S.S.; Abedin, F.; Rahman, K.M. Implementation of an MPPT technique of a solar module with supervised machine learning. *Front. Energy Res.* **2022**, *10*, 932653. [CrossRef]

34. Pradhan, C.; Senapati, M.K.; Ntiakoh, N.K.; Calay, R.K. Roach Infestation Optimization MPPT Algorithm for Solar Photovoltaic System. *Electronics* **2022**, *11*, 927. [CrossRef]
35. Islam, H.; Mekhilef, S.; Shah, N.B.M.; Soon, T.K.; Seyedmahmousian, M.; Horan, B.; Stojcevski, A. Performance evaluation of maximum power point tracking approaches and photovoltaic systems. *Energies* **2018**, *11*, 365. [CrossRef]
36. Torres-Madroñero, J.L.; Nieto-Londoño, C.; Sierra-Pérez, J. Hybrid energy systems sizing for the colombian context: A genetic algorithm and particle swarm optimization approach. *Energies* **2020**, *13*, 5648. [CrossRef]
37. Kennedy, J.; Eberhart, R. Particle swarm optimization. In Proceedings of the ICNN'95—International Conference on Neural Networks, Perth, Australia, 27 November–1 December 1995; Volume 4, pp. 1942–1948.
38. Liu, J.; Zhu, T.; Zhang, Y.; Liu, Z. Parallel Particle Swarm Optimization Using Apache Beam. *Information* **2022**, *13*, 119. [CrossRef]
39. Koad, R.B.; Zobaa, A.F.; El-Shahat, A. A Novel MPPT Algorithm Based on Particle Swarm Optimization for Photovoltaic Systems. *IEEE Trans. Sustain. Energy* **2017**, *8*, 468–476. [CrossRef]
40. Abdali, T.A.N.; Hassan, R.; Muniyandi, R.C.; Aman, A.H.M.; Nguyen, Q.N.; Al-Khaleefa, A.S. Optimized particle swarm optimization algorithm for the realization of an enhanced energy-aware location-aided routing protocol in manet. *Information* **2020**, *11*, 529. [CrossRef]
41. Ishaque, K.; Salam, Z.; Amjad, M.; Mekhilef, S. An improved particle swarm optimization (PSO)-based MPPT for PV with reduced steady-state oscillation. *IEEE Trans. Power Electron.* **2012**, *27*, 3627–3638. [CrossRef]
42. Li, H.; Yang, D.; Su, W.; Lu, J.; Yu, X. An Overall Distribution Particle Swarm Optimization MPPT Algorithm for Photovoltaic System under Partial Shading. *IEEE Trans. Ind. Electron.* **2019**, *66*, 265–275. [CrossRef]
43. Tajuddin, M.F.; Arif, M.S.; Ayob, S.M.; Salam, Z. Perturbative methods for maximum power point tracking (MPPT) of photovoltaic (PV) systems: A review. *Int. J. Energy Res.* **2015**, *39*, 1153–1178. [CrossRef]
44. Swaminathan, N.; Lakshminarasamma, N.; Cao, Y. A Fixed Zone Perturb and Observe MPPT Technique for a Standalone Distributed PV System. *IEEE J. Emerg. Sel. Top. Power Electron.* **2022**, *10*, 361–374. [CrossRef]